American Physiological Society | Physiological Genomics

PUBLISHED ARTICLE
ARCHIVES
SUBSCRIPTIONS
SUBMISSIONS
CONTACT US

Physiol Genomics. Dec 2011; 43(24): 1319–1333.

Published online Sep 27, 2011. doi: 10.1152/physiolgenomics.00048.2011

PMCID: PMC3297084

Panhistone deacetylase inhibitors inhibit proinflammatory signaling pathways to ameliorate interleukin-18-induced cardiac hypertrophy

Gipsy Majumdar,[1] Robert J. Rooney,[2] I. Maria Johnson,[1] and Rajendra Raghow[1,3]

[1]Department of Veterans Affairs Medical Center;

[2]Genome Explorations; and

[3]Department of Pharmacology, University of Tennessee Health Science Center, Memphis, Tennessee

Corresponding author.

Address for reprint requests and other correspondence: R. Raghow, Research Service (151), VA Medical Center, 1030 Jefferson Ave., Memphis TN 38104 (e-mail: wohgarr@cshtu.ude).

Received March 25, 2011; Accepted September 21, 2011.

Abstract

PERTURBATIONS OF METABOLIC homeostasis of the heart by pressure or volume overload or congenital mutations lead to the development of maladaptive cardiac hypertrophy. Cytokines and chemokines that regulate immune/inflammatory pathways appear to be integral to the mechanisms of cardiac hypertrophy; thus, IL-1, TNF-α, and IL-18, elicited in response to ischemia and sepsis, disrupt cardiovascular homeostasis (41, 42, 50, 56, 70). A potential role of IL-18 in cardiac hypertrophy in patients has been corroborated in mice where exogenous administration of IL-18 causes ventricular dysfunction and hypertrophy (73). Furthermore, IL-18 knockout mice elicited a blunted cardiac hypertrophy response to pressure overload (11). The cardiac myocytes exposed to IL-18 also undergo hypertrophy and recapitulate a canonical program of hypertrophy-specific gene expression (7, 40, 73).

Although the molecular bases of maladaptive cardiac response to the congenital or acquired stressors remain poorly defined, there are compelling data to suggest that the altered gene expression seen in hypertrophied heart is regulated by epigenetic remodeling of chromatin (2,18, 19). The architecture of chromatin is dynamically regulated by a number of posttranslational modifications of histones (43). The role of acetylation and deacetylation in chromatin organization and its relationship to transcription have been extensively studied. Reversible lysine acetylation of histone and nonhistone proteins is carried out by histone acetyl transferases (HATs) and histone deacetylases (HDACs). Site-specific acetylation of lysine residues in proteins neutralizes their positive charges that consequently alter their

function (74, 75). The acetylation of histones leads to decondensation of chromatin and its transcriptional activation, whereas inactive chromatin is enriched in deacetylated histones (34, 37). Consistent with this mechanism of chromatin-dependent regulation of gene expression, many transcriptional coactivators (e.g., GCN5, PCAF, CBP/p300) possess HAT activity, whereas HDACs are generally associated with transcriptional repression (34, 37).

HDACs comprise an ancient superfamily of enzymes. The 18 unique mammalian HDACs are categorized into the "classical family" of 11 zinc-dependent hydrolases that are structurally related to the yeast Hda1/Rpd3 proteins and seven "nonclassical" sirtuins that use NAD^+ as a cofactor for enzymatic activity. Based on their phylogeny, domain organization, and subcellular localization, the mammalian HDACs are divided into four classes (44, 75). The members of class I, HDAC1, HDAC2, HDAC3, and HDAC8, contain a central deacetylase domain that is delimited by short NH_2 and COOH termini. Class I HDACs are mainly localized in the nucleus and display high enzymatic activity toward histones. The six members of class II are subgrouped into class IIa (HDAC4, HDAC5, HDAC7, and HDAC9) and class IIb (HDAC6 and HDAC10), possessing one or two catalytic sites, respectively (44, 75). As a solitary member of class IV, HDAC11 is homologous to yeast Rpd3 and Hda1 proteins. The sirtuins comprise class III HDACs (62) and will not be discussed further.

A number of HDACs regulate cardiac gene expression during development and in response to prohypertrophy signals. The heart-specific ablation of HDAC-1 and HDAC-2 genes in mice leads to abnormal development of the heart (48, 66). Similarly, the HDAC-5−/− and HDAC-9−/− mice are hypersusceptible to develop maladaptive cardiac hypertrophy and mice lacking both isoforms develop lethal myocardial defects (9). On the other hand, ectopic expression of constitutively active HDAC-4, -5, and -9 suppressed cardiac hypertrophy in vivo and in vitro (2,68). The myocyte enhancer factor-2 (MEF-2), a transcription factor that dynamically binds to HDACs, plays a key role in cardiac hypertrophy (23, 24, 31). Canonical stressors such as epinephrine or angiotensin II (ANG II) induce phosphorylation of class IIa HDACs and promote their exit from the nucleus. In the absence of nuclear IIa HDACs, MEF-2 recruits HATs to the transcriptional machinery, thus changing it from a transcriptional repressor into a transcriptional activator. Thus subcellular redistribution in response to external signals mechanistically links HDACs to maladaptive cardiac hypertrophy. Consistent with such a mechanism some pan-HDAC inhibitors have been shown to preserve cardiac function in the face of pathological stressors in rodents (21, 24, 33, 40).

We have studied gene expression profiles in the hearts of BALB/c mice eliciting cardiac hypertrophy in response to IL-18, in the presence or absence of pan-HDAC inhibitors (pan-HDACIs). We report that both trichostatin A (TSA) and m-carboxycinnamic acid bis-hydroxamide (CBHA) attenuated IL-18-induced cardiac hypertrophy. Furthermore, we found that an exposure of hearts to IL-18 +/− TSA or CBHA elicited unique signatures of differentially expressed genes (DEGs). Our in silico gene network analysis of the DEGs revealed that both pan-HDACIs opposed proinflammatory signaling pathways elicited by IL-18 to ameliorate cardiac hypertrophy by epigenetic mechanisms that involve chromatin remodeling.

MATERIALS AND METHODS

Materials.

Recombinant IL-18 was purchased from Medical and Biological Laboratories (Woburn, MA). CBHA and TSA were obtained from Merck Research Laboratories and Sigma, respectively. Monospecific antibodies against unmodified histone H3 and histone H3 acetylated at lysine 9 and 18 (K9/18) or triple-methylated at lysine 9 (K9me3) were bought from Santa Cruz. Small interfering RNAs (siRNAs) targeted against phosphatase and tensin homolog (PTEN) were bought from Dharmacon (Lafayette, CO).

Treatments of mice.

Six- to eight-week-old male BALB/c mice (Jackson Laboratories) were used for all experiments. IL-18 (1 μg/mouse/day), CBHA (200 mg/kg/day), TSA (0.5 mg/kg/day)m or combinations of IL-18 with one of the HDACIs were delivered by daily intraperitoneal (IP) injections. The control group of mice received injections of vehicle solution. Cohorts of control and treated animals (8 mice in each group) were anesthetized by intramuscular injections of a mixture of ketamine and xylazine. The hearts and other tissues were processed according to the need of a particular experiment. The delivery of anesthesia and death of mice were carried out according to the protocols approved by the Institutional Animal Care and Use Committee of University of Tennessee Health Science Center/Veterans Affairs Medical Center. All mice were killed on *day 8* after initiation of the treatment, and their total body weights were recorded prior to dissection and removal of their organs. The hearts were removed, trimmed of major vessels, and then rinsed in Hanks' balanced salt solution. After being blotted dry, the tissues were weighed.

Cell culture.

H9c2 cells were purchased from American Type Culture Collection (Bethesda, MD) and were grown in Dulbecco's minimum essential medium containing 10% fetal bovine serum (Hyclone, Logan, UT), 2 mM glutamine, and 1% penicillin-streptomycin. Cells were allowed to reach ~80% confluence in complete culture medium and incubated for additional 24 h in serum-free medium prior to experimental treatments, as outlined previously (40). Replicate cultures of H9c2 cells were incubated in media supplemented with IL-18 (0.1 μg/ml), CBHA (1 μM), or TSA (100 nM).

Quantification of cardiac gene expression.

RNA was extracted from control or treated mouse hearts using TRIzol RNA extraction reagent (Invitrogen Life Technologies). Three distinct layers were formed after addition of chloroform to the tissue extract in TRIzol reagent. Ethanol was added to the aqueous layer to precipitate RNA that was concentrated by centrifugation and dissolved in diethylpyrocarbonate-treated water. The bottom two layers were extracted further to obtain protein (see below). Aliquots of 800 ng of RNA representing control or treated samples were used to synthesize cDNA (SuperScript III, Invitrogen). The relative expression of mRNAs encoding PTEN, atrial natriuretic factor (ANF), skeletal α-actin, desmin, β-myosin heavy chain (MyHC), and α-MyHC from control and treated groups were determined by quantitative real-time PCR (qPCR) using LightCycler480 (Roche). Gene-specific PCR-

primers and TaqMan probes were designed using Universal Probe Library (Roche). The expression of target mRNAs was determined by the Ct method. These data were normalized against 18S ribosomal RNA and were presented as fold changes in treated versus control. Nonspecific PCR amplifications were eliminated by assessing melting curve patterns, as detailed previously (40).

Western blot analysis.

Total cardiac proteins were extracted from the tissue samples used to extract RNA. Two lower layers of the TRIzol extracts were processed to extract protein according to the manufacturer's protocol (Invitrogen Life Technologies). For Western blot analysis, equal amounts of protein from each sample were separated using 10% SDS-PAGE. After electrophoresis, the protein samples were transferred to an Immobilon-P transfer membrane (Millipore, Bedford, MA) using a Trans-Blot electrophoresis transfer cell (Bio-Rad Laboratories, Hercules, CA). The detection and quantification of proteins were done by Western blot using either monoclonal antibodies against PTEN or an anti-phospho-Akt antibody raised in rabbits (Cell Signaling, Beverly, MA). The blots were sequentially reacted with primary antibodies (used after 1:1,000 dilution) followed by horseradish peroxidase-conjugated anti-rabbit IgG antibodies (diluted 1:10,000; Santa Cruz Biotechnology, Santa Cruz, CA). Chemi-luminescence signals developed using ECL Plus kit (Amersham-Pharmacia Biotech, Piscataway, NJ) were quantified as detailed previously (39, 40). The blots probed with PTEN antibodies were stripped and reprobed with an anti-actin antibody (1:10,000) to determine equivalency of protein loading; the blots developed with anti-phospho-Akt were stripped and reprobed with anti-Akt antibody (1:10,000, Cell Signaling) to determine total Akt. The data from three or four replicate experiments were quantified by densitometry, normalized against actin or total Akt, and subjected to statistical analysis.

For analysis of histones, equal amounts of protein from each tissue extract were separated by 15% SDS-PAGE. After electrophoresis, the protein samples were transferred to an Immobilon-P transfer membrane and the proteins on the Western blots were detected by using either mono-specific antibodies (1:3,000) recognizing acetylated (K9/18) or methylated (K9/18) or phosphorylated (S10) histone H3. The blots were reprobed with antibodies against unmodified histone H3 (1:5,000) to determine total histone. The Western blots were subject to densitometry to quantify total and covalently modified histone H3.

Knock-down of PTEN expression with siRNA.

H9c2 cells were seeded in six-well plates in complete culture medium. Cells were serum starved overnight following which cells were incubated with 2 mM of either scrambled siRNA or PTEN targeted siRNA in antibiotic-free complete culture media. Transfection of siRNA was carried out using Dharmafect reagent according to the manufacturer's protocol (Dharmacon, Lafayette, CO), as outlined previously (13, 76). After 12 h, the transfected cells were treated with IL-18 and/or CBHA for additional 48 h. Then total RNA and proteins were extracted as described above and processed for RT-PCR and Western blot analyses, respectively.

Gene expression profiling.

RNA was extracted from mouse hearts by the TRIzol method followed by cleaning up of RNA samples with an RNeasy clean up kit (Qiagen, Valencia, CA). The total yield and quality of RNAs were established by measuring absorbance at 260 nm/280 nm in a spectrophotometer and size-fractionation by electrophoresis in 1% agarose gels, respectively. We used 200 ng aliquots of total RNA per sample for cDNA synthesis using oligo(dT) primer bearing a T7 promoter using ArrayScript. We used Illumina TotalPrep RNA Amplification Kit (Applied Biosystems/Ambion, Austin, TX) for both cDNA and cRNA synthesis. Labeled cRNAs were amplified using MEGAscript in vitro transcription protocol. Aliquots of cRNA from murine hearts were hybridized to Illumina MouseWG-6 v2.0 Expression BeadChip Kits each containing 45,200 murine transcripts from the National Center for Biotechnology Information database (http://www.ncbi.nlm.nih.gov/RefSeq/; build 36, release 22). Microarray chips were hybridized with cRNA at 58°C for 18 h. After being washed and stained, chips were scanned on the Illumina 500GX BeadArray Reader using Illumina BeadScan image data acquisition software (version 3.4.0). The data acquisition, processing, and normalization of the microarray data were done with Illumina BeadStudio GX Module software (version 3.4.0) to generate an output file for statistical analysis. To assess quality metrics of each run, several quality control procedures were implemented. The BeadStudio software generated quality control summary report assessing the performance of the built-in controls in BeadChips across a particular day's runs. Thus analysis allowed us to determine variations in signal intensity, hybridization signal, background signal, and the background-to-noise ratio for all samples analyzed in a given run.

Statistical analyses of differential gene expression.

Statistical, mulitvariate, and clustering analyses were performed in GeneMaths XT (Applied Maths, St-Martens-Latem, Belgium). The identification of differentially expressed genes, derived from probe sets, was based on *1*) Illumina detection values ≥ 0.99 for all samples in at least one experimental or control group, *2*) ANOVA P value ≤ 0.01, and *3*), absolute fold change ≥ 2.0 and independent t-test P value ≤ 0.01 for any experimental group versus its respective control group. Principal component analysis (PCA) was performed using signal values for probe sets with detection values ≥ 0.99 for all samples in at least one experimental or control group; signal values were log2 transformed and standardized by row mean centering prior to PCA. Unsupervised hierarchical clustering of differentially expressed genes was performed by the UPGMA (Unweighted Pair Group Method using Arithmetic averages) method that utilizes Euclidean distance as the similarity metric. Sample clustering was achieved by using complete linkage method with Pearson correlation as the similarity metric. Venn diagrams were generated by Boolean intersection of gene IDs for differentially expressed genes from the indicated pair-wise comparisons.

Bioinformatics analyses.

Gene annotation and Gene Ontology (GO) information were obtained from the National Center for Biotechnology Information (http://www.ncbi.nlm.nih.gov) and the GO Consortium (http://amigo.geneontology.org). Analyses of GO enrichment and KEGG (Kyoto Encyclopedia of Genes and Genomes; http://www.genome.jp/kegg) biochemical pathways were performed using WebGestalt (http://bioinfo.vanderbilt.edu/webgestalt). Additional

pathway analysis was performed using the NCI-Nature Protein Interaction Database (http://pid.nci.nih.gov/). Hypergeometric test *P* values were used to estimate the significance of enrichment of specific GO categories or pathways.

Ingenuity Pathways Analysis.

The canonical network models of differentially expressed genes were developed using the Ingenuity Pathway Analysis (IPA, http://www.ingenuity.com; Ingenuity Systems, Mountain View, CA). An initial gene set of DEGs was first overlaid onto the set of all catalogued interactions and focus genes contained in the IPA library of canonical pathways. The target genes (focus genes) were identified from overrepresented genes in canonical pathways formed by direct interactions with other genes in the initial set. The specificity of a gene's interaction was calculated as the percentage of its interactions with other significant genes in the initial gene set. Genes with highest statistical specificity of connections were used to expand the biological networks of interconnected genes. The Illumina gene lists were uploaded as a text file, and each gene identifier was mapped to its corresponding gene object. To start building networks, the application queries the Ingenuity Pathways Knowledge Base for interactions between Focus Genes and all other gene objects stored in the knowledge base and generates a set of networks each with no more than 35 genes/proteins. IPA then computes a score for each network according to the fit of the user's set of significant genes. The score is derived from a *P* value and indicates the likelihood that the Focus Genes in a network are present due to random chance. The networks graphically denote nodes and edges, or lines (the biological relationships between the nodes). The node symbols used by IPA represent the gene and/or its encoded protein. Assignment of nodes in gene network is made from findings that have been extracted from the scientific literature and stored in the Ingenuity Pathways Knowledge Base. The IPA program assigns a direct connection between two molecules if they are known to physically interact with each other. In contrast, an indirect connection between two molecules is not predicated on physical interaction. The criteria for both direct and indirect connections are derived from published literature, as culled in the Ingenuity Pathways Knowledge Base (http://www.ingenuity.com, Ingenuity Systems). The IPA ranks biological pathways in each network according to their statistical significance (i.e., the number of focus genes represented in the canonical networks). A Fisher's exact test was used to calculate a *P* value predicting the probability that the biological function assigned to that network is explained by chance alone.

RESULTS

IL-18 induces cardiac hypertrophy in mice that is ameliorated by TSA and CBHA.

Woldbaek et al. (73) have reported earlier that BALB/c mice receiving daily IP injections of IL-18 for 7 days developed larger hearts with blunted left ventricle adrenergic response to isoproterenol; IL-18-treated mice also elicited enhanced cardiac expression of phospholamban and ANF. To extend these observations and assess the effect of pan-HDACIs in IL-18-induced cardiac hypertrophy, we gave daily IP injections of vehicle, IL-18, CBHA ,or TSA or combinations of IL-18 with either TSA or CBHA to four cohorts of male BALB/c mice for 7 days. At the end of two independent experiments, we measured the heart and body weights of individual mice in all treatment cohorts. As shown in Fig. 1*A*, IL-

18-treated mice developed larger hearts as indicated by increased heart weight-to-body weight ratios that were significantly normalized by coadministration of either CBHA or TSA. In contrast, the hearts of mice exposed to either CBHA or TSA alone were similar to those of vehicle-treated mice (Fig. 1*A*). The anatomical and histological changes seen in the hearts of IL-18-treated mice were also consistent with the development of cardiac hypertrophy and fibrosis (Fig. 1*B*). The mean ventricular wall thicknesses in IL-18-treated and vehicle-treated mice were 1.6 and 1.1 mm, respectively. Masson's trichrome staining of sections of IL-18-treated hearts revealed that the hypertrophied hearts had larger myocytes interspersed with patches of fibrosis (Supporting Fig. S1).[1] Finally, as shown in Fig. 1*C*, cardiac myocytes of IL-18-treated mice were ~32% larger, and cotreatment of mice with either TSA or CBHA led to a normalization of their myocytes.

A molecular hallmark of cardiac hypertrophy is the re-induction of fetal gene expression that typically involves enhanced cardiac expression of A- and B-type atrial natriuretic factors (ANF and BNF, respectively), and α-skeletal actin and β-MyHC proteins, among others (5, 19). The qPCR data shown in Fig. 2, revealed that IL-18 treatment led to a five- to sevenfold accumulation of mRNAs encoding ANF, skeletal α-actin, β-MyHC, and desmin in the heart with a concomitant decline in the expression of α-MyHC mRNA. This canonical cardiac hypertrophy-specific pattern of gene expression induced by IL-18 was reversed by CBHA (Fig. 2). The opposite actions of IL-18 and CBHA on the expression of α- and β-MyHC and ANF genes were specific since the levels of β-actin or 18S RNA were not significantly changed. A similar action of TSA in switching the expression of α- and β-MyHC and ANF genes has been previously observed in two different models of cardiac hypertrophy. Thus Davis and colleagues (12) showed that in hypothyroid rats eliciting cardiac hypertrophy, TSA upregulated the expression of α-MyHC while concurrently repressing the α- and β-tubulins; TSA-induced improved cardiac contractility was similarly observed in cardiac myocyte, eliciting hypertrophy in response to ANG II. In a related study, phenylephrine-induced hypertrophy in primary rat cardiac myocytes and H9c2 cells was completely reversed by two distinct HDACIs, TSA and SK7041; even more significantly, treatment of cells with either TSA or SK7041 significantly repressed the expression of ANF and β-MyHC genes, canonical manifestations of cardiac hypertrophy in vivo and in vitro (30).

We have reported previously that IL-18-treated H9c2 cardiac myocytes became highly enlarged while they concomitantly elicited induction of a number of cardiac hypertrophy-specific genes, and both physical and molecular manifestations of IL-18-induced hypertrophy were greatly attenuated by CBHA (40). Based on our published data in H9c2 cells, combined with the current observations in BALB/c mice, we posit that IL-18 treatment induces cardiac hypertrophy-specific gene expression in vivo and in vitro that was attenuated by two distinct pan-HDACIs, CBHA and TSA.

Cardiac chromatin of mice exposed to IL-18 and/or HDACIs undergoes remodeling.

The regulation of gene expression underlying normal and abnormal development of heart is intimately associated with dynamic changes in chromatin architecture. Given an essential

role of histones and chromatin remodeling in the heart, we posited that chromatin of cardiac genes was uniquely remodeled in response to pro- and antihypertrophy signals evoked by IL-18 and HDACIs, respectively. To experimentally test this hypothesis, we extracted chromatin from the hearts of vehicle- and/or IL-18/ HDACI-treated mice and analyzed a number of posttranslational modifications of histones by Western blotting. As shown in Fig. 3*A*, in vivo administration of CBHA or TSA induced hyperacetylation of histone H3 at lysine 9 (H3/K9ac) regardless of whether IL-18 was administered or not. In contrast, triple methylation of histone H3 at lysine 9 (H3/K9me3) was enhanced in IL-18-treated hearts, and coadministration of either CBHA or TSA almost completely blocked H3/K9me3 methylation induced by IL-18 (Fig. 3, *B* and *C*). We also carried out a limited analysis of changes in phosphorylation of histone H3 at serine 10 (H3/S10-PO_4) in cardiac chromatin of sentinel mice treated with IL-18 and/or HDACIs. As shown in representative Western blots, IL-18 increased the S10 phosphorylation of histone H3 in the bulk chromatin; either CBHA (Fig. 3*B*) or TSA (Fig. 3*C*) significantly reversed this effect. Treatment with HDACIs alone led to insignificant changes in the (H3/K9me3) methylation or (H3/S10-PO_4) phosphorylation. Based on these observations in intact hearts of BALB/c mice we surmise that the chromatin of cardiac genes is dynamically remodeled by pro- and antihypertrophy signals, in vivo and in vitro. This conclusion is consistent with our chromatin immunoprecipitation (ChIP) data showing that chromatin of a number of cardiac hypertrophy-specific genes (ANF and α- and β-MyHC) in H9c2 cells exposed to IL-18 and/or CBHA was reversibly altered; thus, exposure of H9c2 cells to CBHA led to enhanced acetylation histone H3 (H3/K9) with a concomitant reduction in H3/K9 methylation (40). The precise alterations in the "histone code" of hypertrophy-associated genes in IL-18- and HDACI-treated cells remain to be defined.

Microarray analysis of cardiac gene expression in response to IL-18 and/or HDACIs.

To gain additional insight into the underlying molecular mechanisms by which IL-18 and the pan-HDACIs induced pro- and anticardiac hypertrophy-specific gene expression, respectively, we compared the gene expression profiles in the hearts of control and treated mice. Messenger RNAs from the hearts of eight vehicle-treated mice (control) and from mice receiving IL-18, TSA, or from mice cotreated with IL-18 + TSA (8 in each group) were individually extracted and processed for microarray hybridization. Complementary RNAs from individual mice were hybridized to Illumina MouseWG-6 v2.0 Expression BeadChips, each containing 45,200 transcripts. The hybridization data were filtered using the statistical criteria of absolute ≥1.5 log2 fold change and *P* value of 0.05 to identify subsets of cardiac genes that were differentially regulated in response to different treatment regimens. We also subjected the microarray data obtained from IL-18 ± CBHA and IL-18 ± TSA mice to PCA. The PCA of IL-18 ± TSA experiment, shown in the Supporting Fig. S2, demonstrates that four treatment cohorts occupied unique positions on the PCA graph; vehicle-treated mice and those receiving IP injections of TSA were in close proximity of each other in the PCA. Treatment of the transcriptomic data from the IL-18 ± CBHA cohorts to PCA corroborated what we observed in the IL-18 ± TSA experiment (data not shown).

The analysis of the filtered microarray data sets from individual mice belonging to control and treatment groups (IL-18, TSA and IL-18 + TSA) revealed that although the expression of a vast majority of cardiac genes remained unchanged regardless of the treatment regimen, a subset of 184 genes elicited differential expression in response to IL-18 and/or TSA treatment. Based on their expression characteristics, the DEGs were hierarchically organized into three *clusters A*, *B*, and *C* (Fig. 4). The genes in *cluster A* were not significantly affected by IL-18 or TSA. Conversely, IL-18 and TSA regulated the genes in *clusters B* in an opposite manner; IL-18 generally enhanced the expression of genes in *cluster B*, while TSA significantly suppressed their expression. Finally, a majority of genes in *cluster C* were upregulated by IL-18, and the presence of TSA did not significantly alter their expression (Fig. 4).

Treatment of mice with IL-18 ± CBHA led to the identification of 147 DEGs that also represented three distinct *clusters A, B*, and *C* (Fig. 4). The genes in *clusters A* and *B* were significantly upregulated by IL-18 and downregulated by mice receiving either CBHA or CBHA + IL-18, although the impact of these treatments on genes in *cluster B* was lower. A majority of the genes in *cluster C* was downregulated by IL-18. The pattern of expression of genes in *cluster C* following CBHA treatment, regardless of the presence or absence of IL-18, resembled the pattern seen in saline-treated control hearts (Fig. 4).

To delineate the putative intracellular networks formed by DEGs, initially we parsed 184 genes in *clusters A, B*, and *C* into IL-18-responsive and TSA-responsive subsets and independently analyzed both of these subsets by IPA; the CBHA-responsive genes were similarly analyzed. The IPA of DEGs produced a hierarchical list of focus genes that could be assembled into nodes and edges of canonical gene pathways (Table 1). The two most prominent nodes formed by IL-18-responsive genes were TNF-α (47 connections and 32 focus molecules) and IFNγ (47 network connections with 31 focus molecules). We also noted that DEGs in response to TSA and CBHA elicited a number of common gene networks (e.g., TNF-α- and IFNγ-specific gene networks), although the list of pathways elicited by the two HDACIs is not identical (Table 1). Additional notable networks formed by IL-18-responsive genes (Table 1), in descending order, were NF-κB (38 network connections including 23 focus molecules), phosphatidylinositol 3-kinase (PI3K)-Akt/PKB (43 network connections including 20 focus molecules), IL-6 (40 network connections including 20 focus molecules), STAT1 (34 network connections including 19 focus molecule), hepatocyte nuclear factor (HNF)-4A (24 network connections including 18 focus molecules), and ERK-p38-MAPK. Both TSA- and CBHA-responsive focus genes also formed a number of lesser nodes that included IL-6, NF-κB, STAT1, HNF-4A, and ERK-p38-MAPK (Table 1).

A careful analysis of differentially expressed cardiac genes in response to IL-18 ± TSA revealed that IL-18 induced vast majority of genes connected to the TNF-α-, IFNγ-, NF-κB, and transforming growth factor (TGF)-β-specific gene networks were invariably inhibited by IL-18 ± TSA or CBHA (data not shown). We should note that IL-18 specifically enhanced the expression of a number of chemokines including CCL5, CXCL9, CXCL13, and CXCL16 (Fig. 5*A*); conversely, most of the chemokines were downregulated in the hearts of TSA-treated mice (Fig. 5*B*). Finally, the IPA underscored a key role of PI3K-AKT/PKB-centric signaling mechanisms in the action of IL-18 (Fig. 5*A*) and TSA (Fig. 5*B*).

Since the patterns of cardiac expression of genes in *clusters A, B,* and *C* were cluster specific we also independently analyzed each cluster by IPA. *Cluster A* contains only five genes that were downregulated both by IL-18 and TSA. We found that *cluster B* included 33 genes that were upregulated by IL-18 and formed TNF-α- and NF-κB-specific networks (Fig. 5*C* and Table 2). The IL-18 treatment led to enhanced expression of genes in *cluster B* (Fig. 5*C*) that was dominated by molecules involved in intermediary metabolism (e.g., adiponectin, UCP1/2, SCD, PER2, and ADIG) and cell cycle (e.g., PER, anti-clock, CDKN1A, and CIDEC). In contrast, TSA treatment led to suppression of most of the genes in *cluster B*; these genes formed TNF-α- and p53-specific gene networks, connected to pathways involved in intermediary metabolism and cell cycle regulation (Fig. 5*D* and Table 2). The 146 genes in *cluster C* that were strongly induced by IL-18 but unaffected in the vehicle- or in IL-18 + TSA-treated hearts formed gene networks typical of cytokines (IL-1, IL-2, IL-4, IL-6, IL-10, IL-12, IFNγ, and TNF-α), chemokines (CCL and CXCL), and regulators of immune and inflammatory responses (data not shown).

The 58 genes in *cluster A* that were strongly upregulated by IL-18 but downregulated in the presence of CBHA and IL-18 + CBHA-treated hearts (Fig. 4) were subjected to an IPA program that assembled these genes into five networks. These networks, in descending order, were TNF-α, IFNγ, Ca^{2+}-calmodulin, PI3K/Akt, and MAPK (Table 2). Interestingly, CBHA (regardless of the presence or absence of IL-18) typically downregulated *cluster A*, which consisted of genes involved in regulating immune response in NK and T cells, as exemplified by hematopoietic cell signal transducer (HCST) and C-type lectins 6A and 10A (CLEC6A and CLEC10A), and CCL2 and CCL8 chemokines. The cytoplasmic domain of HCST recruits p85 subunit of PI3K involved in signaling via the receptor complex (HCST-CLEC6A and CLEC10A). The CBHA-responsive subset of genes, many of which depend on PI3K-AKT-PTEN signaling pathways, formed IFNγ-, TNF-α-, and p53-specific gene networks (Table 2, Fig. 5*E*). Thus, the IPA data elucidate that although IL-18 treatment of mice, in the presence of CBHA or TSA, induced unique gene expression profiles, underlying these were a number of common signaling nodes.

The KEGG is a collection of a several databases that incorporate curated genomic information and meld it with known intracellular metabolic pathways and small molecules of biological import. The KEGG analysis converts these molecular interactions and gene networks into biologically functional pathways. Therefore, we subjected IL-18 and TSA-induced DEGs to KEGG analysis (Table 3). The KEGG analyses corroborated the IPA by demonstrating that exposure of heart to IL-18 and HDACIs oppositely affected a number of prominent biological pathways. Evidently, the pro- (IL-18) and anti- (HDACIs) cardiac hypertrophy stimuli affected pathways involved in antigen processing and presentation, nutrient and energy homeostasis, and regulators of cell adhesion, proliferation, and apoptosis (Table 3).

IPA of DEGs revealed that PI3K- and MAPK-specific signaling networks, highly connected to TNF-α-, IFNγ-, and NF-κB-specific pathways, were affected by TSA and CBHA. These signaling pathways strongly impinged on the gene networks implicated in the regulation of intermediary metabolism and cellular energetics [peroxisome proliferator-activated receptor (PPAR) and adipokine signaling]. These data are consistent with the notion that IL-18-

induced cardiac hypertrophy and its mitigation by pan-HDACIs in vitro and in vivo are mechanistically related to Ca^{2+}-calmodulin-PI3K-MAPK-NF-κB signaling pathways.

Validation of a key role of PI3K-AKT-NF-κB signaling in cardiac hypertrophy in vivo and in vitro.

The network analyses of DEGs in the heart strongly corroborated a role of PI3K signaling pathways in the actions of HDACIs. Based on the network analysis and earlier studies showing that IL-18-induced hypertrophy in cardiac myocytes was attenuated by CBHA via its ability to induce PTEN and block PI3K, we hypothesized that HDACIs might reverse IL-18-induced cardiac hypertrophy in vivo by a similar mechanism. To test this hypothesis, we studied expression of PTEN in the hearts of mice on different treatment regimens both at protein and mRNA levels. As shown in Fig. 6*A*, IL-18 had an insignificant effect on the expression of PTEN protein; however, both CBHA and TSA induced a two- to fourfold higher expression of PTEN regardless of the presence or absence of IL-18. The qPCR corroborated the Western blot data by revealing a four- to fivefold induction of PTEN mRNA in response to CBHA ± IL-8 or TSA ± IL-8 (Fig. 6*A*).

H9c2 cardiac myocytes respond to a number of prohypertrophy signals by increasing their size and concomitantly eliciting a canonical program of cardiac hypertrophy-specific gene expression (30, 40). Since CBHA is known to induce a robust expression of PTEN mRNA in H9c2 cells (40), we explored regulation of PTEN expression by HDACIs and how that might affect the PI3-AKT signaling in IL-18-treated H9c2 cells. As shown in Fig. 6*B*, IL-18 induced pAKT in H9c2 cells. Consistent with earlier observations (40), enhanced expression of PTEN in H9c2 cells was elicited by both CBHA and TSA. Additionally, as predicted, a knock-down of PTEN expression by siRNA, regardless of whether cells were treated with IL-18 ± HDACIs, led to enhanced expression of pAKT, the downstream negative target of PTEN. The overall expression of AKT was not significantly affected under these conditions. A hallmark of cardiac hypertrophy is enhanced expression of ANF and β-MyHC that occurs concomitantly with a reduced expression of α-MyHC gene. Consistent with published observations, IL-18 led to an accelerated expression of ANF and β-MyHC genes. Furthermore, we observed that a knock-down of PTEN by siRNA in H9c2 cells led to increased steady-state levels of ANF mRNA and a twofold induction of β-MyHC regardless of whether these cells were incubated with either IL-18 or CBHA (Fig. 6*B*). Although these tantalizing data suggest a potential mechanistic link between PTEN expression and cardiac hypertrophy-specific abnormal expression of ANF and β-MyHC genes, additional experiments are needed to establish this relationship.

DISCUSSION

We examined gene expression profiles in the hearts of BALB/c mice with a goal to shed mechanistic light into IL-18-induced cardiac hypertrophy and its attenuation by HDACIs. In silico examination of the transcriptome data by IPA and KEGG programs revealed that IL-18 in the presence and/or absence of either TSA or CBHA elicited unique gene expression signature in vivo. The genome-wide changes in physiological and pathological hypertrophy have been studied in a number of animal models (16, 20, 26, 28, 69) and in humans (29).

These studies have revealed that an altered immune system, accompanied by changes in cardiac energetics, fat metabolism, oxidative phosphorylation, and cytoskeletal and extracellular matrix, plays a key role in pathological cardiac remodeling (20, 26, 28, 69). Perturbations in the PI3K/AKT and ERK and MAPK cascades have emerged as a dominant theme in the mechanisms of maladaptive cardiac hypertrophy (20, 26, 28, 69). Our network analyses revealed that IL-18 elicited aberrant regulation of gene networks that control immunity and inflammation, cardiac metabolism and energetics, and cell proliferation and apoptosis. Furthermore, in addition to corroborating earlier observations, we demonstrate here that HDACIs counter the pathological gene expression pathways via epigenetic remodeling of cardiac chromatin. Whether the observed actions of HDACIs have analogous effects in other models of cardiac hypertrophy and in humans remains to be established.

It is believed that proinflammatory actions of IL-18 are mediated via induction of IFNγ and TNF-α and chemokines that affect NF-κB signaling (15, 67, 70). Interestingly, IFNγ- and TNF-α-specific gene networks were a recurring theme not only in the intact heart exposed to IL-18 but also in CBHA- or TSA-treated hearts. However, the upregulation of proinflammatory-specific gene networks was potently opposed by HDACIs in vivo. Thus, CXCL16 and CXCL13 chemokines was upregulated by IL-18 and suppressed by TSA. IL-18 has been shown to induce CXCL16 transcription in rat aortic smooth muscle cells via PI3K-Akt-JNK-Ap-1 pathways (8). The involvement of IL-1-, IL-6-, IL-12-, IL-13-, IFNγ-, TGF-β-, and TNF-α-specific gene networks in the hearts exposed to IL-18 was anticipated in light of the known direct and indirect actions of IL-18 on antigen processing and presentation and on metabolic homeostasis (15, 67, 70).

Based on our network analyses we posit that the pathways controlling synthesis and turnover of phosphatidylinositol bis and tris phosphates (IP_2 and IP_3) and their signaling receptors are integral to the mechanisms of IL-18-induced cardiac hypertrophy and its attenuation by HDACIs. The phosphainositide lipid second messengers are involved in intracellular coupling of cardiac myocytes (25). In addition to the involvement of PI3K, a number of prominent kinase (CaM kinase, mTOR, and MAPK)- and phosphatase (calcineurin, MKP)-specific networks were seen in our study; these are known to integrate cellular responses to many stimuli, including IFNγ and TNF-α and chemokines (3, 4, 6, 32, 38, 57, 61). For instance, p38 MAPK regulates not only many aspects of immunity and inflammation, but also the mechanisms that control ANF gene expression, actin reorganization, and growth of cardiac myocytes (26, 57, 58).

With regard to PI3K, it is significant to note that both CBHA and TSA concomitantly induced hyperacetylation of chromatin and PTEN transcription in the heart similarly to what we have previously reported for H9c2 cardiac myocytes (40). We should note, however, that although siRNA knock-down of PTEN led to enhanced expression of pAKT, a direct connection between PI3K-AKT-PTEN pathway and an aberrant expression of ANF and β-MyHC in maladaptive cardiac hypertrophy remains to be experimentally established. Despite the foregoing caveat, our network analyses have corroborated and extended earlier observations (4, 6, 53–55) suggesting that PI3K-PTEN-specific gene pathways engage in cross-talk and feedback regulation by MAPK signaling. Based on the widely recognized role of epigenetic regulatory mechanisms in immunity and inflammation (17), we speculate that

HDACIs counteracted a common step(s) in IL-18-induced signaling pathways to attenuate cardiac hypertrophy.

Both IPA and KEGG pathway analyses revealed that IL-18 had a striking effect on adipokine and PPAR-specific gene networks known to regulate the metabolism of lipids, carbohydrates, amino acids, purines, and pyrimidines, as well as the metabolism of glutathione and xenobiotics. The altered state of metabolic homeostasis in the hearts of IL-18-treated mice was reflected by aberrant expression of SCD, Per2, anti-clock, adiponectin, and UCP-1 and -2 genes. Again, while IL-18 induced expression of adiponectin and UCP1 in the heart, both genes were strongly suppressed by HDACIs. A number of investigators have reported that a major shift in cardiac energetics from fatty acid oxidation to glucose as the main source of fuel occurs in maladaptive cardiac hypertrophy (20, 45, 49, 65, 69). Elevated circulating levels of IL-18 in humans have been implicated in obesity, insulin resistance, and hypertension (67). Paradoxically, however, IL-18−/− mice developed hyperphagia, obesity, and insulin resistance that was accompanied by reduced expenditure of energy (51, 77).

The exposure of hearts to HDACIs in the presence or absence of IL-18 elicited strong gene networks dedicated to the regulation of cell proliferation and death. Our in silico analyses strongly highlighted IFNγ- and TNF-α-specific gene networks that were connected to cyclins and cyclin kinase inhibitors. The two networks were also extensively connected with PI3K and MAPK signaling cascades and transcription factors Myc, p53, NF-κB, and HNF-4A. Both Myc and p53 are known to orchestrate cell cycle and apoptosis in multiple ways (1, 36, 46, 47). The transcription of a number of genes that catalyze S-phase transition is directly enhanced by Myc and p53 while both of these transcription factors concomitantly block expression of genes that regulate cell cycle arrest (1, 36, 46, 47). p53 may also exert an indirect effect on cell cycle of cardiac myocytes due to its ability to impinge on nutrient and energy homeostasis. The activities of Myc and p53 are regulated by chromatin remodeling proteins and other epigenetic modulators (14, 36, 47).

In addition to its key role in liver development during embryogenesis, HNF-4A regulates numerous genes in the adult liver and kidney. The direct downstream targets of HNF-4A include genes that regulate biogenesis and metabolism of glucose, lipids, and proteins (22, 27). Based on its known role in regulating cellular metabolism we postulate that HNF-4A indirectly controls growth, proliferation, and apoptosis of cardiac myocytes in response to treatment with IL-18 and/or HDACIs.

We believe that, in addition to corroborating a key role of a small subset of genes in cardiac homeostasis, our data underscore the concept that maladaptive cardiac hypertrophy and its attenuation by HDACIs also share core gene networks specifying Myc, p53, HNF-4A and NF-κB. This is significant since acetylation and deacetylation are known to modulate the activities of these transcription factors. Furthermore, we provide compelling evidence that these gene networks are subject to feedback regulation by PI3K and MAPK signaling pathways.

Although several clinical trials are currently underway to evaluate the therapeutic potential of pan-HDACIs, the mechanistic underpinnings of how global changes in acetylation of proteins achieve functional selectivity remain largely undefined (34, 49, 52, 59, 60). Recent

application of high-throughput methods that include mass spectrometry-based proteomics, genome-wide ChIP analysis combined with transcriptional profiling have begun to shed mechanistic light into the role of acetylation/deacetylation. These studies have demonstrated that although acetylation is a major covalent modification associated with chromatin, numerous nonhistone proteins are also acetylated; these include transcription factors and metabolic enzymes involved in glycolysis, gluconeogenesis, and fat and glycogen metabolism (10, 35, 49, 52, 60, 63,64, 71, 72). Choudhary et al. (10) identified nearly 1,750 proteins belonging to macromolecular complexes that are known to regulate chromatin remodeling, mRNA biogenesis, nuclear transport, cytoskeleton, and cell cycle in MV4-11, A549, and Jurkat cells exposed to pan-HDACIs MS275 or SAHA (suberoylanilide hydroxamic acid). Thus the structural and functional potential of the human "acetylome" more than rivals that of all other posttranslational modifications discovered to date.

In summary, the genome-wide analyses of actions of CBHA and TSA in the intact heart and in H9c2 cells, as probed by IPA and KEGG, have provided a glimpse into the mechanisms by which HDACIs selectivity inhibit postinflammatory signaling mechanisms by blocking the PI3K pathway via induction of PTEN.

GRANTS

The research carried out in our laboratory was supported by the DVA and the National Institutes of Health; a research enhancement program grant from the DVA partially supported G. Majumdar's research.

DISCLOSURES

No conflicts of interest, financial or otherwise, are declared by the author(s).

AUTHOR CONTRIBUTIONS

Author contributions: G.M. and R.R. conception and design of research; G.M. and I.M.J. performed experiments; G.M., R.J.R., and I.M.J. analyzed data; G.M., R.J.R., and R.R. interpreted results of experiments; G.M., R.J.R., and I.M.J. prepared figures; G.M. drafted manuscript; G.M. and R.R. edited and revised manuscript; R.R. approved final version of manuscript.

ACKNOWLEDGMENTS

We acknowledge technical assistance of Neha Bhargava in these studies. Thoughtful discussions with Professor Ivan Gerling greatly benefitted our IPA data analyses. R. Raghow is a Senior Research Career Scientist of the Department of Veterans Affairs (DVA).

Footnotes

[1]The online version of this article contains supplemental material.

REFERENCES

1. Ak P, Levine AJ. p53 and NF-kappaB: different strategies for responding to stress lead to a functional antagonism. FASEB J 24: 3643–3652, 2010. [PubMed: 20530750]
2. Backs J, Olson EN. Control of cardiac growth by histone acetylation/deacetylation. Circ Res 98: 15–24, 2006. [PubMed: 16397154]
3. Barki-Harrington L, Perrino C, Rockman HA. Network integration of the adrenergic system in cardiac hypertrophy. Cardiovasc Res 63: 391–402, 2004. [PubMed: 15276464]
4. Bers DM. Calcium cycling and signaling in cardiac myocytes. Annu Rev Physiol 70: 23–49, 2008. [PubMed: 17988210]
5. Braunwald E, Bristow MR. Congestive heart failure: fifty years of progress. Circulation 102: IV14–IV23, 2000. [PubMed: 11080127]
6. Carracedo A, Pandolfi PP. The PTEN-PI3K pathway: of feedbacks and cross-talks. Oncogene 27: 5527–5541, 2008. [PubMed: 18794886]
7. Chandrasekar B, Mummidi S, Claycomb WC, Mestril R, Nemer M. Interleukin-18 is a pro-hypertrophic cytokine that acts through a phosphatidylinositol 3-kinase-phosphoinositide-dependent kinase-1-Akt-GATA4 signaling pathway in cardiomyocytes. J Biol Chem 280: 4553–4567, 2005. [PubMed: 15574430]
8. Chandrasekar B, Mummidi S, Valente AJ, Patel DN, Bailey SR, Freeman GL, Hatano M, Tokuhisa T, Jensen LE. The pro-atherogenic cytokine interleukin-18 induces CXCL16 expression in rat aortic smooth muscle cells via MyD88, interleukin-1 receptor-associated kinase, tumor necrosis factor receptor-associated factor 6, c-Src, phosphatidylinositol 3-kinase, Akt, c-Jun N-terminal kinase, and activator protein-1 signaling. J Biol Chem 280: 26263–26277, 2005. [PubMed: 15890643]
9. Chang S, McKinsey TA, Zhang CL, Richardson JA, Hill JA, Olson EN. Histone deacetylases 5 and 9 govern responsiveness of the heart to a subset of stress signals and play redundant roles in heart development. Mol Cell Biol 24: 8467–8476, 2004. [PMCID: PMC516756][PubMed: 15367668]
10. Choudhary C, Kumar C, Gnad F, Nielsen ML, Rehman M, Walther TC, Olsen JV, Mann M. Lysine acetylation targets protein complexes and co-regulates major cellular functions. Science 325: 834–840, 2009. [PubMed: 19608861]
11. Colston JT, Boylston WH, Feldman MD, Jenkinson CP, de la Rosa SD, Barton A, Trevino RJ, Freeman GL, Chandrasekar B. Interleukin-18 knockout mice display maladaptive cardiac hypertrophy in response to pressure overload. Biochem Biophys Res Commun 354: 552–558, 2007. [PMCID: PMC1847636] [PubMed: 17250807]
12. Davis FJ, Pillai JB, Gupta M, Gupta MP. Concurrent opposite effects of trichostatin A, an inhibitor of histone deacetylases, on expression of alpha-MHC and cardiac tubulins: implication for gain in cardiac muscle contractility. Am J Physiol Heart Circ Physiol 288: H1477–H1490, 2005. [PubMed: 15388503]
13. Deng X, Yellaturu C, Cagen L, Wilcox HG, Park EA, Raghow R, Elam MB. Expression of the rat sterol regulatory element-binding protein-1c gene in response to insulin is mediated by increased transactivating capacity of specificity protein 1 (Sp1). J Biol Chem 282: 17517–17529, 2007. [PubMed: 17449871]
14. Dey A, Lane DP, Verma CS. Modulating the p53 pathway. Semin Cancer Biol 20: 3–9, 2010. [PubMed: 20193765]
15. Dinarello CA. Interleukin 1 and interleukin 18 as mediators of inflammation and the aging process. Am J Clin Nutr 83: 447S–455S, 2006.[PubMed: 16470011]

16. Drozdov I, Tsoka S, Ouzounis CA, Shah AM. Genome-wide expression patterns in physiological cardiac hypertrophy. BMC Genomics11: 557, 2010. [PMCID: PMC3091706] [PubMed: 20937113]
17. Dubovsky JA, Villagra A, Powers JJ, Wang HW, Pinilla-Ibarz J, Sotomayor EM. Circumventing immune tolerance through epigenetic modification. Curr Pharm Des 16: 268–276, 2010. [PubMed: 20109136]
18. Frey N, Katus HA, Olson EN, Hill JA. Hypertrophy of the heart: a new therapeutic target? Circulation 109: 1580–1589, 2004.[PubMed: 15066961]
19. Frey N, Olson EN. Cardiac hypertrophy: the good, the bad, and the ugly. Annu Rev Physiol 65: 45–79, 2003. [PubMed: 12524460]
20. Galindo CL, Skinner MA, Errami M, Olson LD, Watson DA, Li J, McCormick JF, McIver LJ, Kumar NM, Pham TQ, Garner HR.Transcriptional profile of isoproterenol-induced cardiomyopathy and comparison to exercise-induced cardiac hypertrophy and human cardiac failure. BMC Physiol 9: 23, 2009. [PMCID: PMC2799380] [PubMed: 20003209]
21. Gallo P, Latronico MV, Grimaldi S, Borgia F, Todaro M, Jones P, Gallinari P, De Francesco R, Ciliberto G, Steinkuhler C, Esposito G, Condorelli G. Inhibition of class I histone deacetylase with an apicidin derivative prevents cardiac hypertrophy and failure. Cardiovasc Res80: 416–424, 2008. [PubMed: 18697792]
22. Gonzalez FJ. Regulation of hepatocyte nuclear factor 4 alpha-mediated transcription. Drug Metab Pharmacokinet 23: 2–7, 2008.[PubMed: 18305369]
23. Haberland M, Arnold MA, McAnally J, Phan D, Kim Y, Olson EN. Regulation of HDAC9 gene expression by MEF2 establishes a negative-feedback loop in the transcriptional circuitry of muscle differentiation. Mol Cell Biol 27: 518–525, 2007. [PMCID: PMC1800816][PubMed: 17101791]
24. Haberland M, Montgomery RL, Olson EN. The many roles of histone deacetylases in development and physiology: implications for disease and therapy. Nat Rev Genet 10: 32–42, 2009. [PMCID: PMC3215088] [PubMed: 19065135]
25. Hofgaard JP, Banach K, Mollerup S, Jorgensen HK, Olesen SP, Holstein-Rathlou NH, Nielsen MS. Phosphatidylinositol-bisphosphate regulates intercellular coupling in cardiac myocytes. Pflügers Arch 457: 303–313, 2008 [PMCID: PMC3727395]
26. Isserlin R, Merico D, Alikhani-Koupaei R, Gramolini A, Bader GD, Emili A. Pathway analysis of dilated cardiomyopathy using global proteomic profiling and enrichment maps. Proteomics 10: 1316–1327, 2010. [PMCID: PMC2879143] [PubMed: 20127684]
27. Kamiyama Y, Matsubara T, Yoshinari K, Nagata K, Kamimura H, Yamazoe Y. Role of human hepatocyte nuclear factor 4alpha in the expression of drug-metabolizing enzymes and transporters in human hepatocytes assessed by use of small interfering RNA. Drug Metab Pharmacokinet 22: 287–298, 2007. [PubMed: 17827783]
28. Kang BY, Hu C, Ryu S, Khan JA, Biancolella M, Prayaga S, Seung KB, Novelli G, Mehta P, Mehta JL. Genomics of cardiac remodeling in angiotensin II-treated wild-type and LOX-1-deficient mice. Physiol Genomics 42: 42–54, 2010. [PubMed: 20332185]
29. Kaufman BD, Desai M, Reddy S, Osorio JC, Chen JM, Mosca RS, Ferrante AW, Mital S. Genomic profiling of left and right ventricular hypertrophy in congenital heart disease. J Card Fail 14: 760–767, 2008. [PubMed: 18995181]

30. Kee HJ, Kook H. Kruppel-like factor 4 mediates histone deacetylase inhibitor-induced prevention of cardiac hypertrophy. J Mol Cell Cardiol 47: 770–780, 2009. [PubMed: 19729022]
31. Kim Y, Phan D, van Rooij E, Wang DZ, McAnally J, Qi X, Richardson JA, Hill JA, Bassel-Duby R, Olson EN. The MEF2D transcription factor mediates stress-dependent cardiac remodeling in mice. J Clin Invest 118: 124–132, 2008. [PMCID: PMC2129240][PubMed: 18079970]
32. Kok K, Geering B, Vanhaesebroeck B. Regulation of phosphoinositide 3-kinase expression in health and disease. Trends Biochem Sci 34: 115–127, 2009. [PubMed: 19299143]
33. Kong Y, Tannous P, Lu G, Berenji K, Rothermel BA, Olson EN, Hill JA. Suppression of class I and II histone deacetylases blunts pressure-overload cardiac hypertrophy. Circulation 113: 2579–2588, 2006. [PMCID: PMC4105979] [PubMed: 16735673]
34. Kouzarides T. Chromatin modifications and their function. Cell 128: 693–705, 2007. [PubMed: 17320507]
35. Lee KK, Workman JL. Histone acetyltransferase complexes: one size doesn't fit all. Nat Rev Mol Cell Biol 8: 284–295, 2007.[PubMed: 17380162]
36. Levine AJ, Oren M. The first 30 years of p53: growing ever more complex. Nat Rev Cancer 9: 749–758, 2009. [PMCID: PMC2771725][PubMed: 19776744]
37. Li B, Carey M, Workman JL. The role of chromatin during transcription. Cell 128: 707–719, 2007. [PubMed: 17320508]
38. Long YC, Glund S, Garcia-Roves PM, Zierath JR. Calcineurin regulates skeletal muscle metabolism via coordinated changes in gene expression. J Biol Chem 282: 1607–1614, 2007. [PubMed: 17107952]
39. Majumdar G, Harrington A, Hungerford J, Martinez-Hernandez A, Gerling IC, Raghow R, Solomon S. Insulin dynamically regulates calmodulin gene expression by sequential o-glycosylation and phosphorylation of sp1 and its subcellular compartmentalization in liver cells. J Biol Chem 281: 3642–3650, 2006. [PubMed: 16332679]
40. Majumdar G, Johnson IM, Kale S, Raghow R. Epigenetic regulation of cardiac muscle-specific genes in H9c2 cells by Interleukin-18 and histone deacetylase inhibitor m-carboxycinnamic acid bis-hydroxamide. Mol Cell Biochem 312: 47–60, 2008. [PubMed: 18292970]
41. Mallat Z, Corbaz A, Scoazec A, Graber P, Alouani S, Esposito B, Humbert Y, Chvatchko Y, Tedgui A. Interleukin-18/interleukin-18 binding protein signaling modulates atherosclerotic lesion development and stability. Circ Res 89: E41–E45, 2001. [PubMed: 11577031]
42. Mallat Z, Heymes C, Corbaz A, Logeart D, Alouani S, Cohen-Solal A, Seidler T, Hasenfuss G, Chvatchko Y, Shah AM, Tedgui A.Evidence for altered interleukin 18 (IL)-18 pathway in human heart failure. FASEB J 18: 1752–1754, 2004. [PubMed: 15371332]
43. Martin C, Zhang Y. Mechanisms of epigenetic inheritance. Curr Opin Cell Biol 19: 266–272, 2007. [PubMed: 17466502]
44. Martin M, Kettmann R, Dequiedt F. Class IIa histone deacetylases: regulating the regulators. Oncogene 26: 5450–5467, 2007.[PubMed: 17694086]

45. McMullen JR, Jennings GL. Differences between pathological and physiological cardiac hypertrophy: novel therapeutic strategies to treat heart failure. Clin Exp Pharmacol Physiol 34: 255–262, 2007. [PubMed: 17324134]
46. Menendez D, Inga A, Resnick MA. The expanding universe of p53 targets. Nat Rev Cancer 9: 724–737, 2009. [PubMed: 19776742]
47. Meyer N, Penn LZ. Reflecting on 25 years with MYC. Nat Rev Cancer 8: 976–990, 2008. [PubMed: 19029958]
48. Montgomery RL, Davis CA, Potthoff MJ, Haberland M, Fielitz J, Qi X, Hill JA, Richardson JA, Olson EN. Histone deacetylases 1 and 2 redundantly regulate cardiac morphogenesis, growth, and contractility. Genes Dev 21: 1790–1802, 2007. [PMCID: PMC1920173][PubMed: 17639084]
49. Montgomery RL, Potthoff MJ, Haberland M, Qi X, Matsuzaki S, Humphries KM, Richardson JA, Bassel-Duby R, Olson EN.Maintenance of cardiac energy metabolism by histone deacetylase 3 in mice. J Clin Invest 118: 3588–3597, 2008. [PMCID: PMC2556240][PubMed: 18830415]
50. Naito Y, Tsujino T, Fujioka Y, Ohyanagi M, Okamura H, Iwasaki T. Increased circulating interleukin-18 in patients with congestive heart failure. Heart 88: 296–297, 2002. [PMCID: PMC1767350] [PubMed: 12181230]
51. Netea MG, Joosten LA, Lewis E, Jensen DR, Voshol PJ, Kullberg BJ, Tack CJ, van Krieken H, Kim SH, Stalenhoef AF, van de Loo FA, Verschueren I, Pulawa L, Akira S, Eckel RH, Dinarello CA, van den Berg W, van der Meer JW. Deficiency of interleukin-18 in mice leads to hyperphagia, obesity and insulin resistance. Nat Med 12: 650–656, 2006. [PubMed: 16732281]
52. Nightingale KP, Gendreizig S, White DA, Bradbury C, Hollfelder F, Turner BM. Cross-talk between histone modifications in response to histone deacetylase inhibitors: MLL4 links histone H3 acetylation and histone H3K4 methylation. J Biol Chem 282: 4408–4416, 2007.[PubMed: 17166833]
53. O'Neill BT, Kim J, Wende AR, Theobald HA, Tuinei J, Buchanan J, Guo A, Zaha VG, Davis DK, Schell JC, Boudina S, Wayment B, Litwin SE, Shioi T, Izumo S, Birnbaum MJ, Abel ED. A conserved role for phosphatidylinositol 3-kinase but not Akt signaling in mitochondrial adaptations that accompany physiological cardiac hypertrophy. Cell Metab 6: 294–306, 2007. [PMCID: PMC2084219][PubMed: 17908558]
54. Odom DT, Zizlsperger N, Gordon DB, Bell GW, Rinaldi NJ, Murray HL, Volkert TL, Schreiber J, Rolfe PA, Gifford DK, Fraenkel E, Bell GI, Young RA. Control of pancreas and liver gene expression by HNF transcription factors. Science 303: 1378–1381, 2004.[PMCID: PMC3012624] [PubMed: 14988562]
55. Oudit GY, Kassiri Z, Zhou J, Liu QC, Liu PP, Backx PH, Dawood F, Crackower MA, Scholey JW, Penninger JM. Loss of PTEN attenuates the development of pathological hypertrophy and heart failure in response to biomechanical stress. Cardiovasc Res 78: 505–514, 2008. [PubMed: 18281373]
56. Rabkin SW. The role of interleukin 18 in the pathogenesis of hypertension-induced vascular disease. Nat Clin Pract Cardiovasc Med 6: 192–199, 2009. [PubMed: 19234499]
57. Raman M, Chen W, Cobb MH. Differential regulation and properties of MAPKs. Oncogene 26: 3100–3112, 2007. [PubMed: 17496909]

58. Rohini A, Agrawal N, Koyani CN, Singh R. Molecular targets and regulators of cardiac hypertrophy. Pharmacol Res 61: 269–280, 2010.[PubMed: 19969085]
59. Ruthenburg AJ, Li H, Patel DJ, Allis CD. Multivalent engagement of chromatin modifications by linked binding modules. Nat Rev Mol Cell Biol 8: 983–994, 2007. [PubMed: 18037899]
60. Saha A, Wittmeyer J, Cairns BR. Chromatin remodelling: the industrial revolution of DNA around histones. Nat Rev Mol Cell Biol 7: 437–447, 2006. [PubMed: 16723979]
61. Schieven GL. The p38alpha kinase plays a central role in inflammation. Curr Top Med Chem 9: 1038–1048, 2009. [PubMed: 19747121]
62. Schwer B, Verdin E. Conserved metabolic regulatory functions of sirtuins. Cell Metab 7: 104–112, 2008. [PubMed: 18249170]
63. Spange S, Wagner T, Heinzel T, Kramer OH. Acetylation of non-histone proteins modulates cellular signalling at multiple levels. Int J Biochem Cell Biol 41: 185–198, 2009. [PubMed: 18804549]
64. Sterner DE, Berger SL. Acetylation of histones and transcription-related factors. Microbiol Mol Biol Rev 64: 435–459, 2000.[PMCID: PMC98999] [PubMed: 10839822]
65. Strom CC, Aplin M, Ploug T, Christoffersen TE, Langfort J, Viese M, Galbo H, Haunso S, Sheikh SP. Expression profiling reveals differences in metabolic gene expression between exercise-induced cardiac effects and maladaptive cardiac hypertrophy. FEBS J 272: 2684–2695, 2005. [PubMed: 15943803]
66. Trivedi CM, Luo Y, Yin Z, Zhang M, Zhu W, Wang T, Floss T, Goettlicher M, Noppinger PR, Wurst W, Ferrari VA, Abrams CS, Gruber PJ, Epstein JA. Hdac2 regulates the cardiac hypertrophic response by modulating Gsk3 beta activity. Nat Med 13: 324–331, 2007.[PubMed: 17322895]
67. Troseid M, Seljeflot I, Arnesen H. The role of interleukin-18 in the metabolic syndrome. Cardiovasc Diabetol 9: 11, 2010.[PMCID: PMC2858122] [PubMed: 20331890]
68. Vega RB, Harrison BC, Meadows E, Roberts CR, Papst PJ, Olson EN, McKinsey TA. Protein kinases C and D mediate agonist-dependent cardiac hypertrophy through nuclear export of histone deacetylase 5. Mol Cell Biol 24: 8374–8385, 2004. [PMCID: PMC516754][PubMed: 15367659]
69. Wagner RA, Tabibiazar R, Powers J, Bernstein D, Quertermous T. Genome-wide expression profiling of a cardiac pressure overload model identifies major metabolic and signaling pathway responses. J Mol Cell Cardiol 37: 1159–1170, 2004. [PubMed: 15572046]
70. Wang M, Markel TA, Meldrum DR. Interleukin 18 in the heart. Shock 30: 3–10, 2008. [PubMed: 18562922]
71. Wang Q, Zhang Y, Yang C, Xiong H, Lin Y, Yao J, Li H, Xie L, Zhao W, Yao Y, Ning ZB, Zeng R, Xiong Y, Guan KL, Zhao S, Zhao GP. Acetylation of metabolic enzymes coordinates carbon source utilization and metabolic flux. Science 327: 1004–1007, 2010.[PubMed: 20167787]
72. Wang Z, Zang C, Cui K, Schones DE, Barski A, Peng W, Zhao K. Genome-wide mapping of HATs and HDACs reveals distinct functions in active and inactive genes. Cell 138: 1019–1031, 2009. [PMCID: PMC2750862] [PubMed: 19698979]

73. Woldbaek PR, Sande JB, Stromme TA, Lunde PK, Djurovic S, Lyberg T, Christensen G, Tonnessen T. Daily administration of interleukin-18 causes myocardial dysfunction in healthy mice. Am J Physiol Heart Circ Physiol 289: H708–H714, 2005.[PubMed: 15821032]
74. Yang XJ, Seto E. Lysine acetylation: codified crosstalk with other posttranslational modifications. Mol Cell 31: 449–461, 2008.[PMCID: PMC2551738] [PubMed: 18722172]
75. Yang XJ, Seto E. The Rpd3/Hda1 family of lysine deacetylases: from bacteria and yeast to mice and men. Nat Rev Mol Cell Biol 9: 206–218, 2008. [PMCID: PMC2667380] [PubMed: 18292778]
76. Yellaturu CR, Deng X, Park EA, Raghow R, Elam MB. Insulin enhances the biogenesis of nuclear sterol regulatory element-binding protein (SREBP)-1c by posttranscriptional down-regulation of Insig-2A and its dissociation from SREBP cleavage-activating protein (SCAP). SREBP-1c complex. J Biol Chem 284: 31726–31734, 2009. [PMCID: PMC2797243] [PubMed: 19759400]
77. Zorrilla EP, Sanchez-Alavez M, Sugama S, Brennan M, Fernandez R, Bartfai T, Conti B. Interleukin-18 controls energy homeostasis by suppressing appetite and feed efficiency. Proc Natl Acad Sci USA 104: 11097–11102, 2007. [PMCID: PMC1904154] [PubMed: 17578927]

Figures and Tables

Fig. 1.

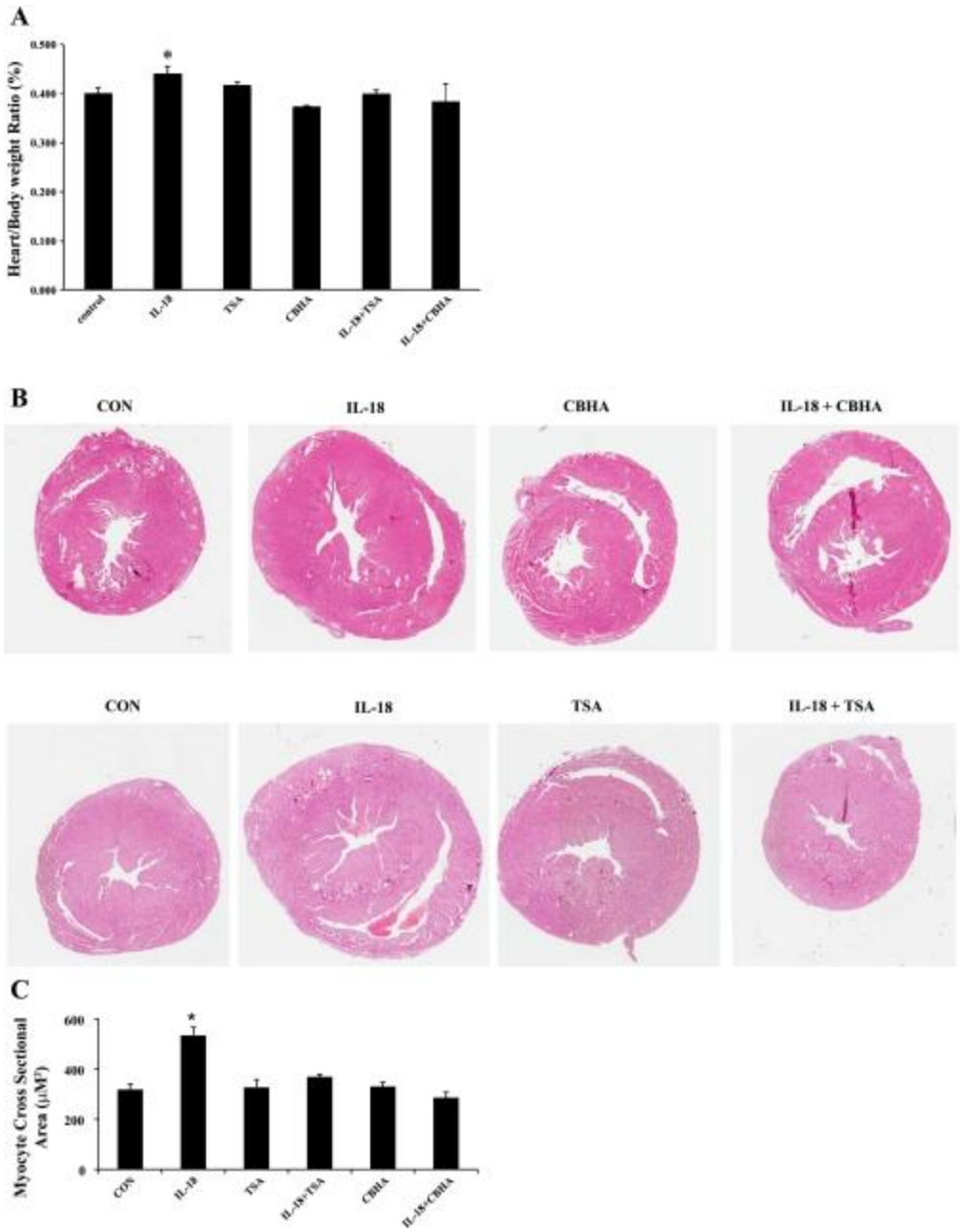

Parameters of cardiac hypertrophy in mice treated with IL-18 ± trichostatin A (TSA) or m-carboxycinnamic acid bis-hydroxamide (CBHA). Mice were injected daily with IL-18 in the presence and absence of TSA or CBHA and were killed on the 8th day. *A*: heart weight-to-body weight (HW/BW) ratios. The hearts were removed, trimmed, and weighed separately; the ratios of HW/BW were calculated for each mouse. Values are means ± SE; $n = 10$ mice in each treatment group. *$P < 0.05$ vs. control. *B*: cardiac histology in mice treated with IL-18 ± TSA or CBHA. Hearts from the vehicle (CON)- and IL-18-treated mice in the presence and absence of either TSA or CBHA were fixed with paraformaldehyde; the paraffinized sections of heart were stained with hematoxylin and eosin (H&E). *C*: changes in myocyte sizes in mice treated with IL-18 ± TSA or CBHA. The myocyte sizes were quantified from cardiac sections stained with H&E at a magnification of ×400. Transverse areas of myocytes through the transmural regions of the left ventricle were quantified with 50 cells per slide using a hemocytometer-calibrated measuring ruler of the Imagescope software. Values are means ± SE and *$P < 0.01$ vs. control.

Fig. 2.

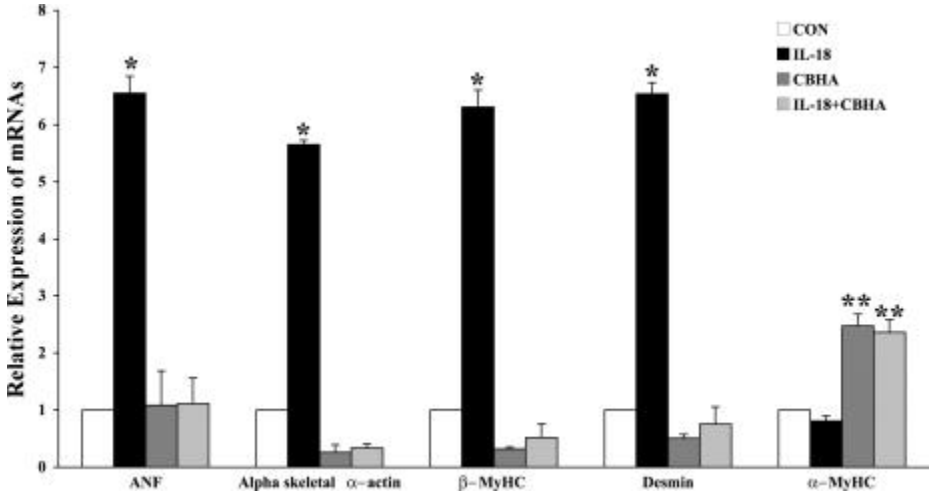

Cardiac hypertrophy-specific gene expression in response to IL-18 ± CBHA. Total RNA from the hearts of mice receiving vehicle or IL-18 ± CBHA for 7 days were extracted with TRIzol reagent and analyzed by qPCR. IL-18 triggered enhanced cardiac accumulation of mRNAs encoding atrial natriuretic factor (ANF), skeletal α-actin, desmin, and β-myosin heavy chain (MyHC). CBHA treatment attenuated the expression of all these transcripts. The mRNAs were quantified in individual mice heart in each treatment group (4 mice/group). The data were normalized against 18S ribosomal RNA and were expressed as fold change over the control (CON). Values are means ± SE; *$P < 0.01$ vs. control, **$P < 0.05$ vs. control.

Fig. 3.

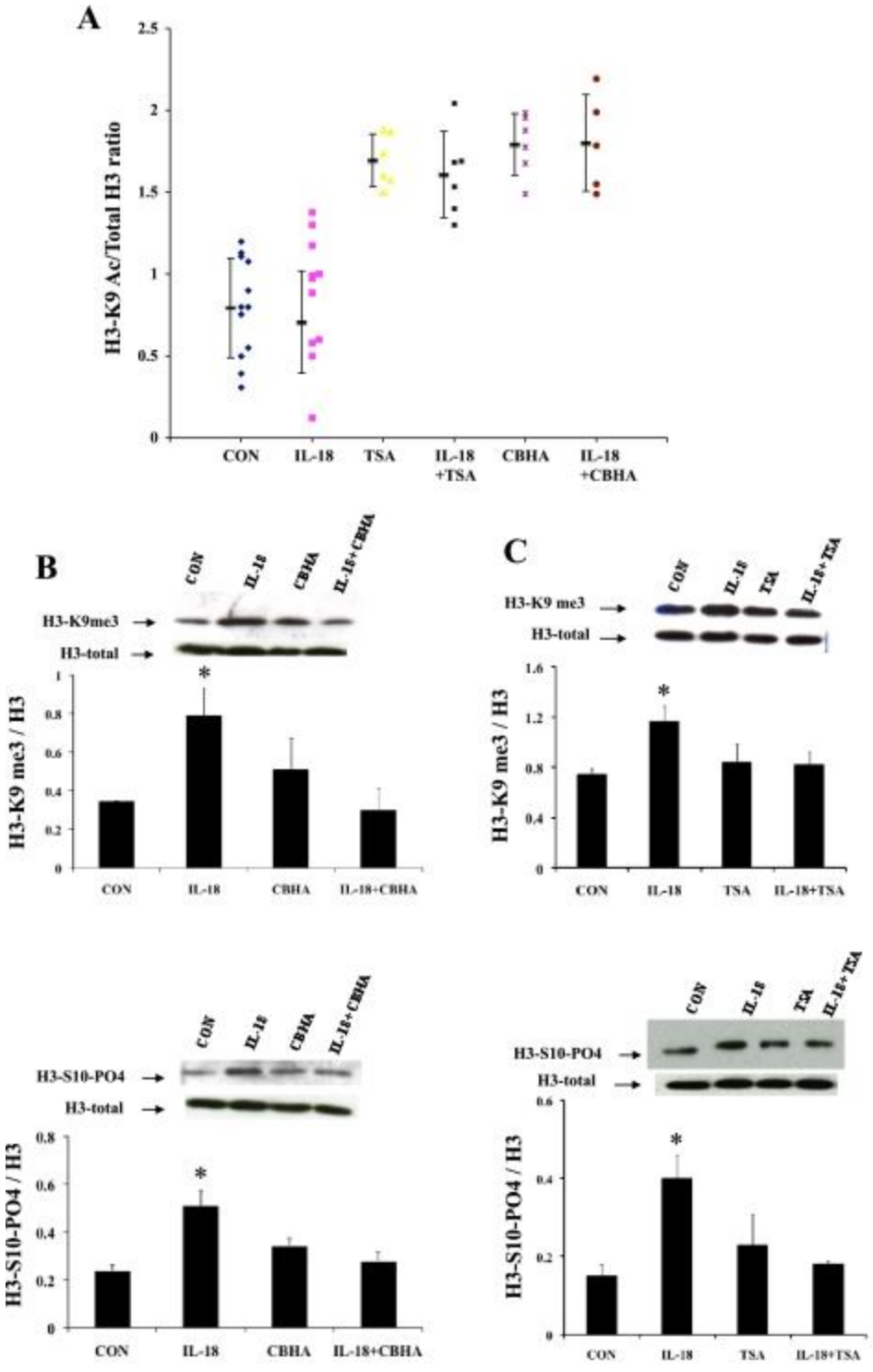

Posttranslational modifications of histones in the cardiac chromatin of mice treated with IL-18 ± TSA or CBHA. Mice were injected with IL-18 with or without CBHA or TSA. We separated 3 μg aliquots of protein extracts from individual mouse heart by 15% SDS-PAGE. Western blots were sequentially probed with mono-specific antibodies against histone H3-K9ac, H3-K9me3, or H3-S10-PO_4, or unmodified histone H3. *A*: acetylation of histone H3 (H3-K9) in mice treated with IL-18 ± CBHA or TSA. A ratio of acetylated H3-K9 to total histone H3 in cardiac chromatin of mice representing different treatment

cohorts was calculated by densitometry. Each point represents data from an individual mouse heart. Values are shown as means (horizontal bar) ± SD. *P* values of TSA, CBHA, TSA + IL-18, CBHA + IL-18 vs. CON are $P < 0.05$. *B*: methylation (H3-K9me3) and phosphorylation (H3-S10-PO_4) of histone H3 in mice treated with IL-18 ± CBHA. Representative Western blots of total, H3-K9me3, and H3-S10-PO_4, and quantification by densitometry of 3 independent immunoblots are shown. A ratio of methylated H3-K9me3 (top) or phosphorylated H3-S10-PO_4 (bottom) to total histone H3 was calculated. Values are ± SE; $*P < 0.05$ vs. CON. *C*: methylation (H3-K9m3) and phosphorylation (H3-S10-PO_4) of histone H3 in mice treated with IL-18 ± TSA. Representative Western blots of total, H3-K9me3, and H3-S10-PO_4 and quantification by densitometry of 3 independent immunoblots are shown. A ratio of methylated H3-K9m3 (top) or phosphorylated H3-S10-PO_4 (bottom) to total histone H3 was calculated. Values are ± SE; $*P < 0.05$ vs. control.

Fig. 4.

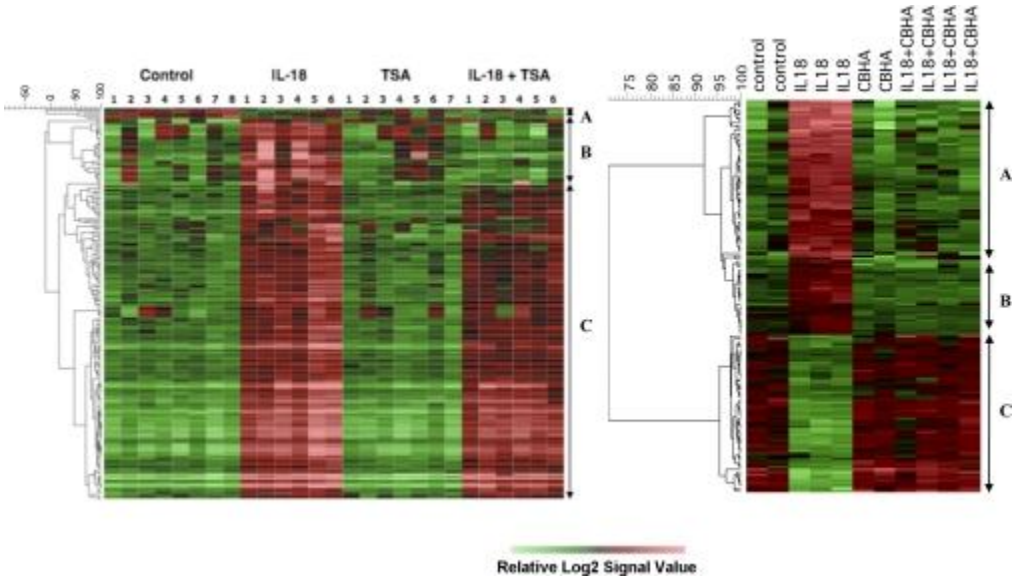

Clustered heat maps of differentially expressed genes (DEGs) in the hearts of mice in response to IL-18 in the presence or absence of TSA or CBHA. The unsupervised hierarchical clusterings of 184 DEGs (*left*) or 147 DEGs (*right*) are depicted as heat maps created as described in MATERIALS AND METHODS. These data sets were filtered for significant differential expression based on Illumina detection values (>0.99 for all samples for at least 1 group), 1.5-fold change in treatment vs. CON group, ANOVA *P* values (<0.05), and *t*-test *P* values (<0.05). Based on their unique expression characteristics DEGs comprise 3 clusters, A, B, and C.

Table 1.

Key cytokine and signaling pathways elicited in the heart in response to IL-18 or TSA/CBHA in mice

Control vs. IL-18	Control vs. TSA	Control vs. CBHA

Gene Pathway	Total Connections (focus genes, *n*)	Gene Pathway	Total Connections (focus genes, *n*)	Gene Pathway	Total Connections (focus genes, *n*)
TNF	47 (32)	TNF	69 (45)	TNF	41 (14)
IFNγ	47 (31)	IFNγ	68 (42)	TGF-β	40 (14)
NF-κB	38 (23)	IL-6	62 (38)	calcium	38 (14)
PI3K-Akt	43 (20)	NF-κB	56 (33)	HNF4α	21 (14)
IL-6	40 (20)	TGF-β1	56 (31)	IFNG	37 (12)
STAT1	34 (19)	PI3K-Akt	63 (21)	TP53	34 (10)
HNF-4A	24 (18)	STAT1	33 (20)	MYC	39 (8)
ERK	26 (11)	HNF-4A	25 (20)	PI3K-Akt	38 (8)
P38MAPK	26 (10)	ERK	33 (13)	NF-κB	36 (7)

Control vs. IL-18		Control vs. TSA		Control vs. CBHA	
Gene Pathway	**Total Connections (focus genes, *n*)**	**Gene Pathway**	**Total Connections (focus genes, *n*)**	**Gene Pathway**	**Total Connections (focus genes, *n*)**
TGF-β1	32 (8)	P38MAPK	27 (10)	ERK	30 (7)
AP1	22 (7)	JNK	29 (9)	JNK	25 (7)
JNK	22 (6)	CDKN1A	35 (7)	P38-MAPK	26 (5)

A total of 184 differentially expressed genes (DEGs) in *clusters A, B*, and *C* (Fig. 4) in response to IL-18 or trichostatin (TSA) were analyzed by Ingenuity Pathway Analysis (IPA) as described in MATERIALS AND METHODS. Similarly, 147 DEGs (Fig. 4) in response to m-carboxycinnamic acid bis-hydroxamide (CBHA) were also subjected to IPA. The gene pathways are arranged in descending order according to the number of focus genes connected to the main node.

Fig. 5.

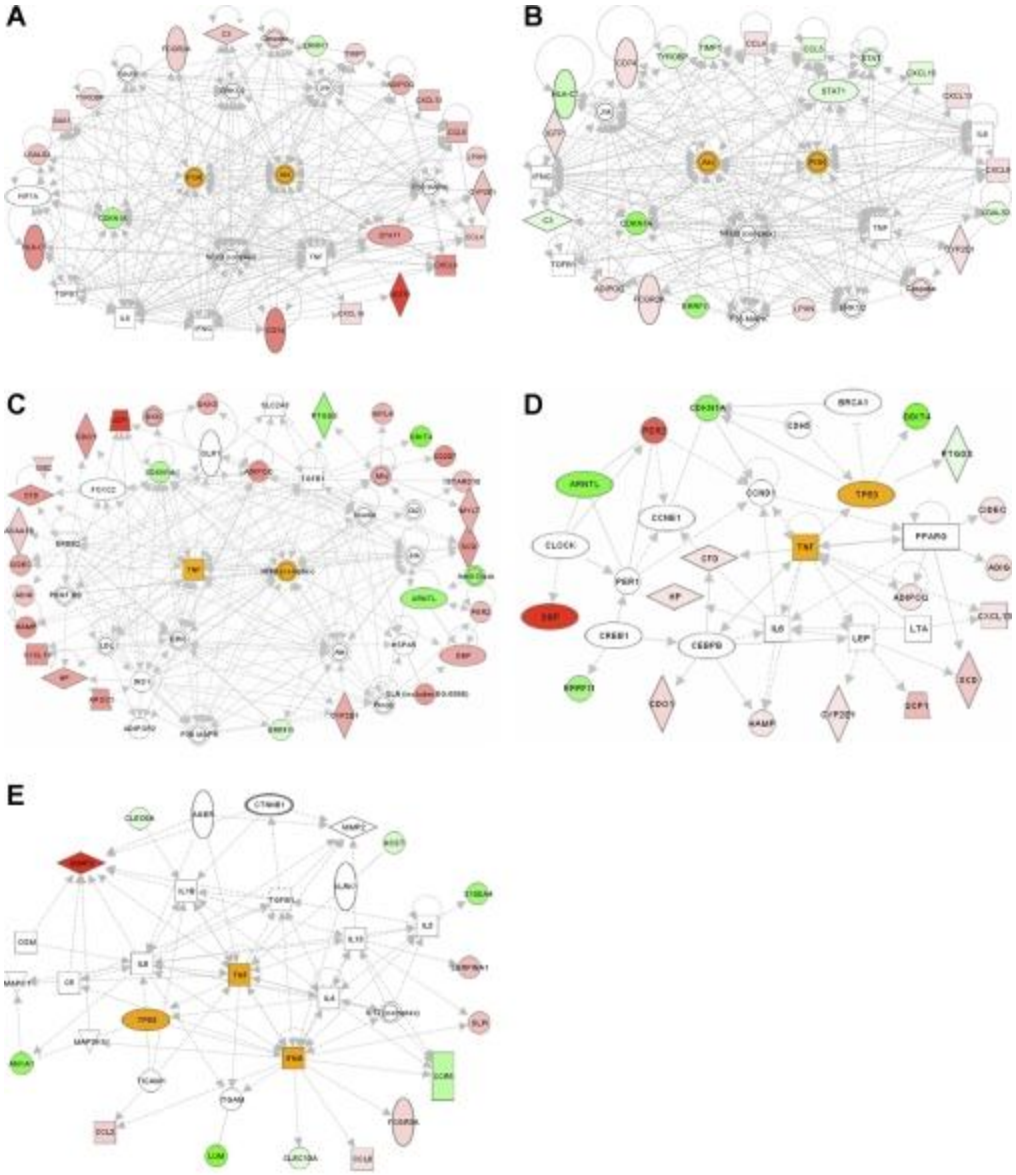

Common intracellular signaling pathways affected by IL-18 ± TSA or CBHA. *A*: a vast majority of genes, induced by IL-18 (colored red), are connected to phosphatidylinositol 3-kinase (PI3K)- and AKT-specific networks either directly (solid lines) or indirectly (broken lines) The Ingenuity Pathway Analysis (IPA) program assigns a direct connection between 2 molecules if they are known to have a physical interaction; for example, AKT directly interacts with ERK but indirectly with CDKN1A in the gene networks. *B*: TSA-responsive genes forming PI3K- and AKT-specific gene networks. In contrast to IL-18, TSA strongly (green) or moderately (pink) downregulated most of these transcripts. *C*: the subset for IL-18-responsive 38 genes contained in *clusters A* and *B* (Fig. 4) formed central nodes of TNF-α and NF-κB that are connected to insulin, PI3K-AKT, and p38MAPK pathways. *D*: the TSA-responsive cardiac genes contained in*clusters A* and *B* formed strong TNF-α- and TP53-specific nodes that were either upregulated (pink and red) or downregulated (green). *E*: the IFNγ, TNF-α, and TP53-specific gene networks formed by CBHA-responsive cardiac genes in *cluster A*.

Table 2.

The main gene networks formed by DEGs in clusters A and B regulated by IL-18 and TSA or CBHA

Control vs. IL-18		**Control vs. TSA**		**Control vs. CBHA**	
Gene Pathway	**Total Connections (focus genes, *n*)**	**Gene Pathway**	**Total Connections (focus genes, *n*)**	**Gene Pathway**	**Total Connections (focus genes, *n*)**
TNF	26 (8)	TNF	12 (3)	IFNγ	19 (5)
ERBR2	19 (6)	TP53	6 (3)	TNF	14 (1)
TGF-β	25 (5)	IL-6	9 (2)	TGF-β	10 (1)
NF-κB	17 (5)	cyclin D	6 (2)	TP53	4 (1)
Akt	15 (4)	CDKN1A	5 (1)		
P38-MAPK	15 (4)	cyclin E	4 (1)		
ERK	15 (3)				

Control vs. IL-18		Control vs. TSA		Control vs. CBHA	
Gene Pathway	**Total Connections (focus genes, *n*)**	**Gene Pathway**	**Total Connections (focus genes, *n*)**	**Gene Pathway**	**Total Connections (focus genes, *n*)**
JNK	13 (3)				
Insulin	12 (3)				

A total of 38 genes that elicited differential expression in response to IL-18 or TSA and 58 DEGs specific for CBHA were subjected to IPA as detailed in MATERIALS AND METHODS. Gene pathways with total number of connections (direct and indirect) and focus molecules are arranged in a descending order.

Table 3.

The KEGG pathways represented by DEGs in the heart of mice treated with IL-18 and/or TSA

KEGG Pathway	Gene nos.	Entrez Gene IDs	*P* Value
Antigen processing and presentation	12	MHC11, H2-Ab1, H2-Ea, HLA_DM, HLA-DB1, H2-Eb1, PA28 MHC1, TAPBP, TAP1, TAP2, GILT	4.26e-17
Cell adhesion molecules (CAMs)	9	MHC11, H2-Ab1, H2-Ea, HLA_DM, HLA-DB1, H2-Eb1, MHC1, SIGLEC1, PD-L1	1.13e-9

KEGG Pathway	Gene nos.	Entrez Gene IDs	*P* Value
Cytokine-cytokine receptor interaction	9	CCR5, CXC9, CCL4, CCL5, CCL7, CCL9, CXCL13 CXCL16, IL-1	1.91e-7
Type I diabetes mellitus	6	H2-Ab1, H2-D1, H2-Ea, HLA-DM, HLA-DB1, H2-Eb1, IL-1, INS	8.33e-12
Toll-like receptor signaling pathway	5	IL-1, CXCL9 CCL4 CCL5, STAT1	1.71e-5
Complement and coagulation cascades	4	DF, C1Q, C2, C3	8.41e-5
PPAR signaling pathway	3	Adipoq, SCD1, UCP1	2.06e-3
Hematopoietic cell lineage	3	H2-ea, H2-eb1, IL-1	3.03e-3
Natural killer cell-mediated cytotoxicity	3	Fcrg111, 14964 DAPI	7.62e-3
Leukocyte transendothelial	3	NCF4, CXCL13, CXCL16	7.81e-3

KEGG Pathway	Gene nos.	Entrez Gene IDs	*P* Value
migration			
Arachidonic acid metabolism	2	CYP2E, Ptdgs	2.41e-2
Circadian rhythm	2	PER, Arntl	9.94e-4
ABC transporters - general	2	ABCB2, ABCB3	9.32e-3
MAPK signaling pathway	2	BDNF, IL-1	2.51e-1
Adipocytokine signaling pathway	1	Adipoq	2.28e-1

The KEGG pathways are hierarchically arranged based on the number of DEGs. The Entrez Gene IDs and *P* values indicating the significance of enrichment calculated from the hypergeometric test as outlined in MATERIALS AND METHODS are also shown. The KEGG analysis for DEGs generated by IL-18 and/or CBHA is similar to that shown in the table but the Gene IDs are not identical.

Fig. 6.

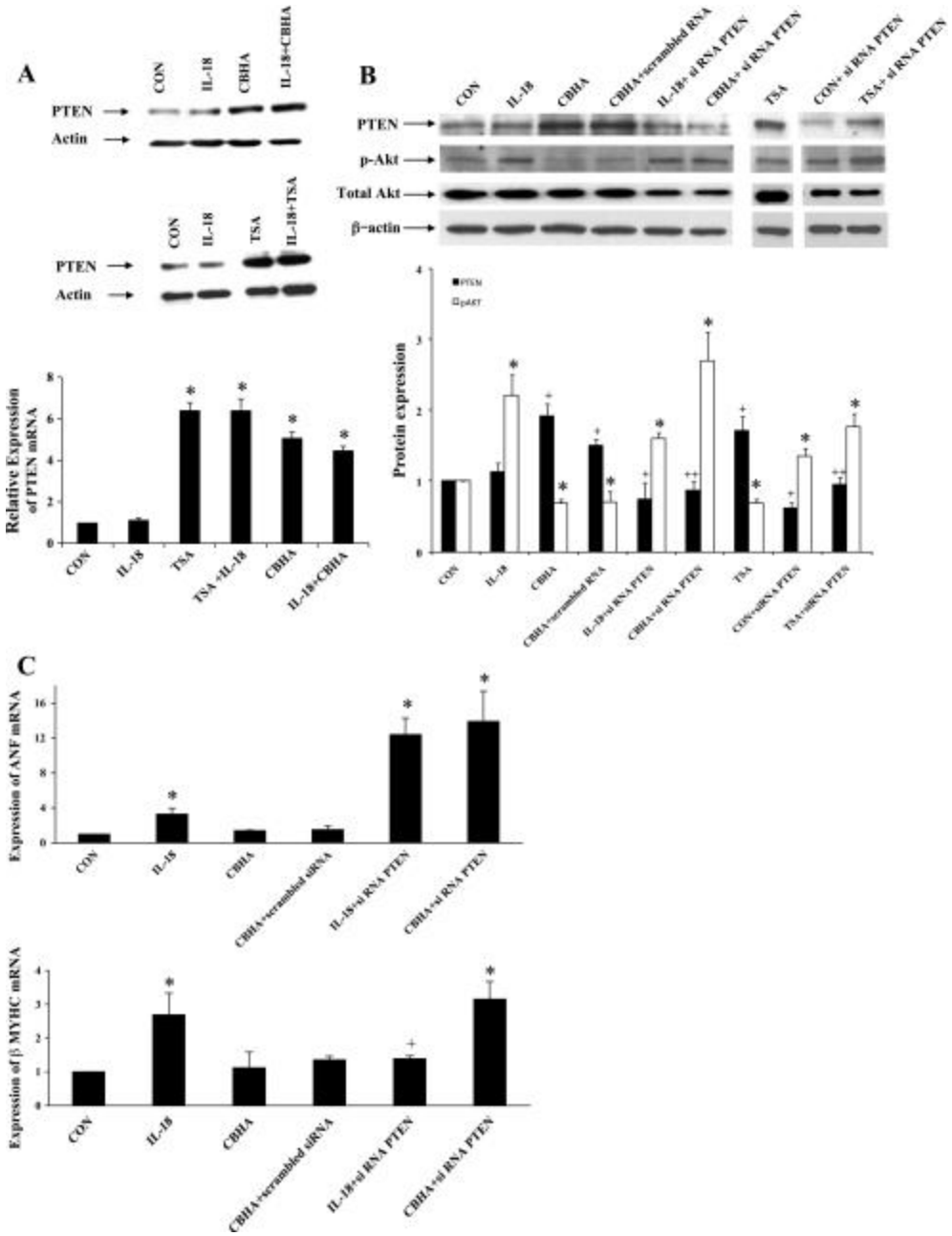

Cardiac expression of phosphatase and tensin homolog (PTEN) in vivo and in vitro. *A*: PTEN expression following IL-18 treatment in mice with or without TSA or CBHA. Total RNA and proteins were extracted from the CON and treated mice using TRIzol reagent. We separated 10 μg of protein extracts from mouse heart by SDS-PAGE. Proteins transferred to the membrane were detected by anti-PTEN antibody. Blots were washed and reprobed with anti-actin antibody. Representative Western blots of PTEN in response to either IL-18 ± CBHA or TSA (*top*). The Western blot representing TSA experiment was assembled from duplicate experiments. The space between lanes representing CON and IL-18 (*left* 2 lanes) and *right* 2 lanes (TSA and IL-18 + TSA) indicates that these lanes were spliced from different locations in the Western blot. The mRNAs encoding PTEN from control and TSA or CBHA-treated groups were quantified by qPCR. The results of qPCR from 3 independent experiments, performed in triplicate each time, are shown (*bottom*). Values are means ± SE; $*P < 0.05$ vs. control. *B*: knock-down of PTEN gene expression with siRNA. H9c2 cells were transfected with 2 mM of either scrambled siRNA

or PTEN siRNA. After 12 h, the transfected cells were treated with IL-18 ± TSA or CBHA for additional 48 h. Protein extracts from H9c2 cells were separated by SDS-PAGE, transferred to the membrane, and sequentially probed with anti-PTEN and anti phospho-Akt (pAKT) antibodies. Finally, blots were also probed with anti-total Akt and anti-actin antibodies. The CBHA experiment (*lanes 1–6*) and the TSA experiment (*lanes 7–9*) were carried out at 2 different times. Spacing between *lane 7* (TSA) and *lanes 8* and *9* (CON + siRNA PTEN and TSA + siRNA PTEN, respectively) indicates splicing of different lanes. Representative Western blots of PTEN and pAkt (*top*) and quantification by densitometry of 3 independent immunoblots are shown (*bottom*). Values are ± SE; **P* < 0.05 vs. control; ^{+}P < 0.05 vs. control; ^{++}P < 0.05 vs. CBHA or TSA. *C*: knock-down of PTEN gene expression with siRNA leads to altered expression of cardiac hypertrophy-specific-genes. H9c2 cells transfected with either scrambled siRNA or PTEN targeted siRNA were treated with IL-18 ± TSA or CBHA for 48 h. Total RNA was analyzed for steady-state levels of mRNA encoding ANF and β-MyHC by qPCR using specific primer pairs. The results of qPCR from 3 independent experiments, performed in triplicate each time, are shown. Values are means ± SE; **P* < 0.05 vs. control and +*P* < 0.03 vs. IL-18.
